Examination of circulation, flushing time and dispersion in Halifax Harbour of Nova Scotia

Shiliang Shan and Jinyu Sheng

ABSTRACT

This study examines the circulation, flushing time and hydrodynamic connectivity in Halifax Harbour based on three-dimensional currents produced by a multi-nested coastal ocean circulation modelling system. The time-mean currents produced by the modelling system feature two-layer estuarine circulation with a seaward flow in the upper layer and a landward flow in the lower layer in the Harbour. The hydrodynamics in the Harbour are also affected significantly by tides and wind forcing. Based on numerical passive tracer experiments, the estimated e-folding flushing time is about 40 and 90 days in the upper and the entire Bedford Basin, respectively. By comparison, the flushing time is about 2–5 days over the Inner and Outer Harbour, and only about 1 day in the Narrows. Analysis of passive particle trajectories carried by the model currents demonstrates that movements of particles in the Harbour are strongly affected by tidal and storm-induced currents. Hydrodynamic connectivity in the study region is also quantified in terms of a connectivity matrix calculated from particle trajectories.

Key words | flushing time, Halifax Harbour, hydrodynamic connectivity, numerical model, particle tracking, tracer

Shiliang Shan (corresponding author)
Jinyu Sheng
Department of Oceanography,
Dalhousie University,
Halifax,
Nova Scotia,
Canada
E-mail: *sshan@phys.ocean.dal.ca*

INTRODUCTION

Halifax Harbour is a large natural harbour on the south coast of Nova Scotia, Canada, facing the North Atlantic Ocean. The Harbour is also an estuary with a small river at the Harbour head (Figure 1). Geographically, Halifax Harbour can be divided into five regions: Bedford Basin, the Narrows, Northwest Arm, Inner Harbour and Outer Harbour. There are significant activities in the Harbour, including a naval base, oil refinery, power station, Halifax Port, ship building yard, and several sewage treatment plants (STPs). The increasing population in the Halifax area indirectly increases the volume of sewage piped into the Harbour. Untreated sewage and wastewater has been flushed into Halifax Harbour through several outfalls for centuries. A new STP was constructed and began operation in February 2008, leading to a significant improvement of the water quality in the Harbour. However, the STP was shut down in January 2009 due to an extended local area power outage and multiple mechanical malfunctions. As a result, raw sewage was again discharged directly into the Harbour. The STP was back online on 24 June 2010. Nevertheless, during intense precipitation periods associated with storms, the combined sewers, including raw untreated sewage and storm water, could exceed the processing capacity of the STP and are only screened and pumped directly into the Harbour.

The sewage discharge and other human activities have created many environmental problems in Halifax Harbour. For example, an area of ~90 km^2 in the Harbour was closed to shellfish harvesting due to high bacterial concentrations of Harbour waters, resulting in $27 million in Canadian dollars of lost revenue between 1965 and 2000 (Wilson 2000). Floatable waste not only causes aesthetic offence, but is also a hazard to some marine animals. The long-term dumping of sewage into Halifax Harbour has also resulted in the buildup of deposits of organic contaminants, heavy metals and toxic and hazardous

doi: 10.2166/wqrjc.2012.041

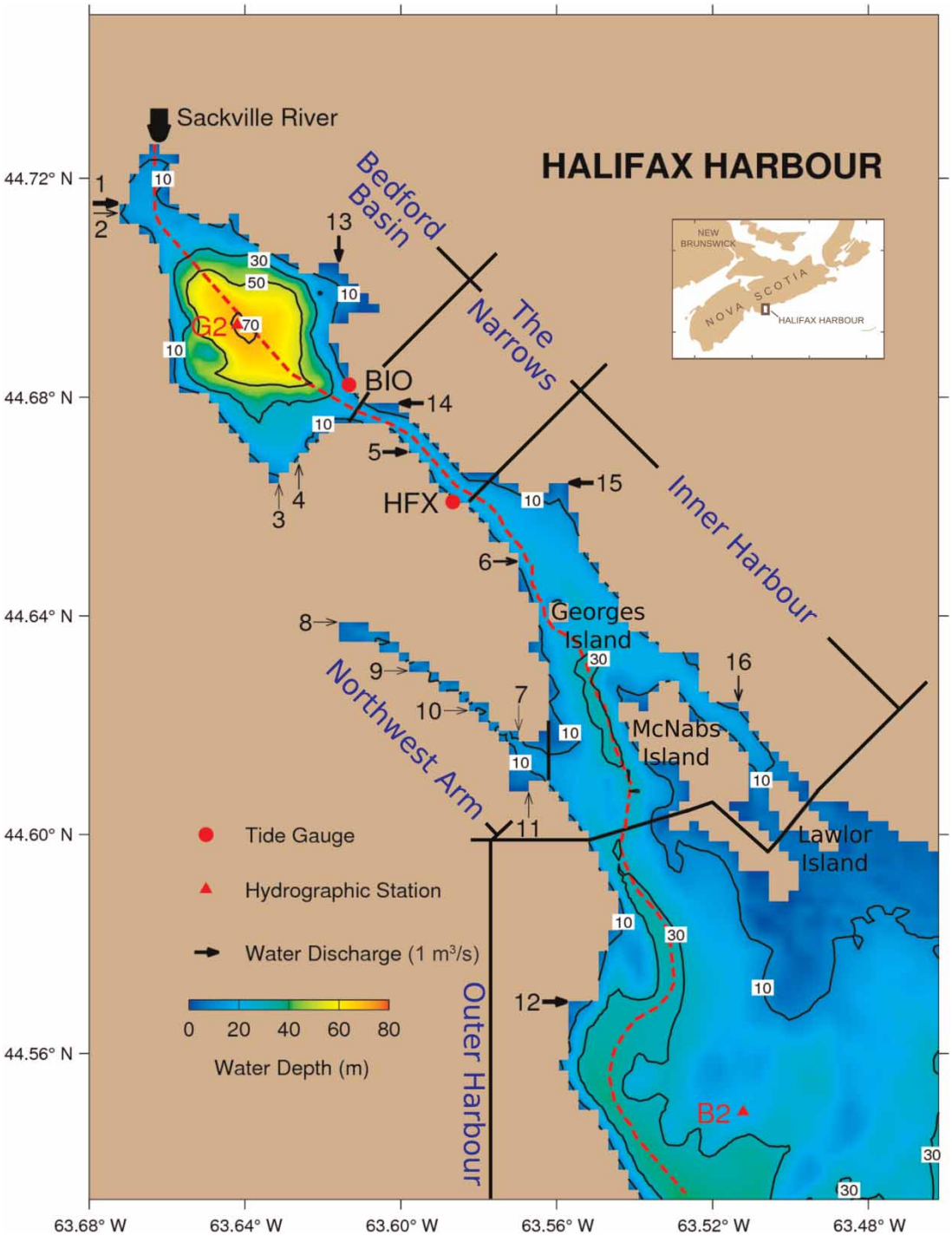

Figure 1 | Bathymetry and geographic features of Halifax Harbour and adjacent waters. Five geographic divisions labelled in blue are used in this study. Red dots indicate positions of two Canadian Hydrographic Service (CHS) tide gauges: CHS station 490 near the Naval Dockyard (HFX) and CHS station 491 near the Bedford Institute of Oceanography (BIO). Red triangles represent positions of two hydrographic stations: G2 in Bedford Basin and B2 in the Outer Harbour. Water discharge locations are numbered 1 to 16 and discharge values are indicated by scaled arrows. The thick bold arrow at the head of Bedford Basin represents the climatological annual mean discharge (1971–2007) of the Sackville River, about 5.04 $m^3 s^{-1}$. The red dashed line represents a transect from the mouth of the Sackville River through Bedford Basin following the deep channel to the open sea. This transect is used in the discussion of the annual mean circulation and passive tracer experiments. Please refer to the online version of this paper to see this figure in colour: http://www.iwaponline.com/wqrjc/toc.htm. With kind permission from Springer Science + Business Media: (Shan *et al*. (2011), Figure 1).

chemicals in the sediments (Fournier 1990; Buckley & Winters 1992).

Circulation plays a fundamental role in advecting and dispersing wastewater and particles in coastal waters. Numerical models have been widely used to study the role of circulation, tidal currents in particular, on the water exchange and dispersion in the coastal region. For example, Signell & Butman (1992) studied tidal exchange and dispersion in Boston Harbour using a two-dimensional circulation model. Choi & Lee (2004) described a method to determine the flushing time via numerical tracer experiments and applied the method to several tidal inlets in Hong Kong. Sheng *et al*. (2009) numerically examined the circulation and hydrodynamic connectivity in Lunenburg Bay of Nova Scotia. Ali *et al*. (2011) investigated the organic waste dispersion from fjord located fish farms using a circulation model with a particle tracking routine.

Circulation in Halifax Harbour has been studied through observations and numerical simulations. The earliest field study of the circulation in the Harbour was made by Huntsman (1924). Based on a simple box model, Petrie & Yeats (1990) demonstrated that the mean circulation of the Harbour is a classical two-layer estuarine circulation. They also used the same box model to study the distribution of heavy metals, suspended solids and nutrient distributions in the Harbour. Most recently a multi-nested coastal ocean circulation modelling system (DalCoast-HFX) was developed by Shan *et al*. (2011) for simulating the three-dimensional (3D) circulation and hydrographic distributions in the Harbour. They demonstrated that DalCoast-HFX accurately reproduces the main features of the observed tides and storm surge, seasonal mean two-layer estuarine circulation, and wind driven variations in the Harbour and adjacent waters.

A better knowledge of major physical processes, flushing time and dispersion in Halifax Harbour is needed to predict the possible pollution effects of sewage discharge. Reliable prediction of water movement is also essential for an effective ecosystem-based management of natural resources in the region. This is a companion paper to Shan *et al*. (2011). The main objective of this study is to numerically examine the flushing time and dispersion in Halifax Harbour based on the concentrations of passive tracers and trajectories of passive particles carried by the time-dependent, 3D currents produced by DalCoast-HFX.

The structure of this paper is as follows. First, the coastal ocean circulation modelling system for Halifax Harbour is described, including the governing equations for calculating concentrations of passive tracers and trajectories of passive particles from simulated 3D currents. Model validation and a series of tracer and particle tracking experiments are then presented, and the flushing time and hydrodynamic connectivity in the Harbour are quantified based on the experimental results. The final section is a summary and discussion.

THE MULTI-NESTED MODELLING SYSTEM

Circulation model

The circulation model used in this study is the multi-nested coastal circulation modelling system for Halifax Harbour (DalCoast-HFX) developed by Shan *et al*. (2011). The modelling system has five submodels (Figure 2) with a coarse horizontal resolution (1/12°) outer-most model for the eastern Canadian shelf and a fine horizontal resolution (~200 m) inner-most model for Halifax Harbour, Bedford Basin and adjacent waters. DalCoast-HFX is based on the Princeton Ocean Model (POM, submodels L1–L2) and CANDIE (submodels L3–L5) (Sheng *et al*. 1998; Thompson *et al*. 2007; Yang & Sheng 2008). The one-way nesting technique is used to transfer information from an upper-level to a lower-level submodel. The subgrid scale horizontal mixing parameterization used in the model is the shear and grid size dependent scheme of Smagorinsky (1963). The vertical mixing schemes of Mellor & Yamada (1982) and Durski *et al*. (2004) are used in submodels L1–L2 and submodels L3–L5, respectively. The multi-nested modelling system is forced by tides, winds, surface heat fluxes and freshwater discharges. A more detailed description of the external forcing and boundary conditions used in DalCoast-HFX can be found in Shan *et al*. (2011). The model is initialized from a state of rest with the December monthly mean density climatology and integrated for 13 months, from December 2005 to December 2006. The simulated time-dependent

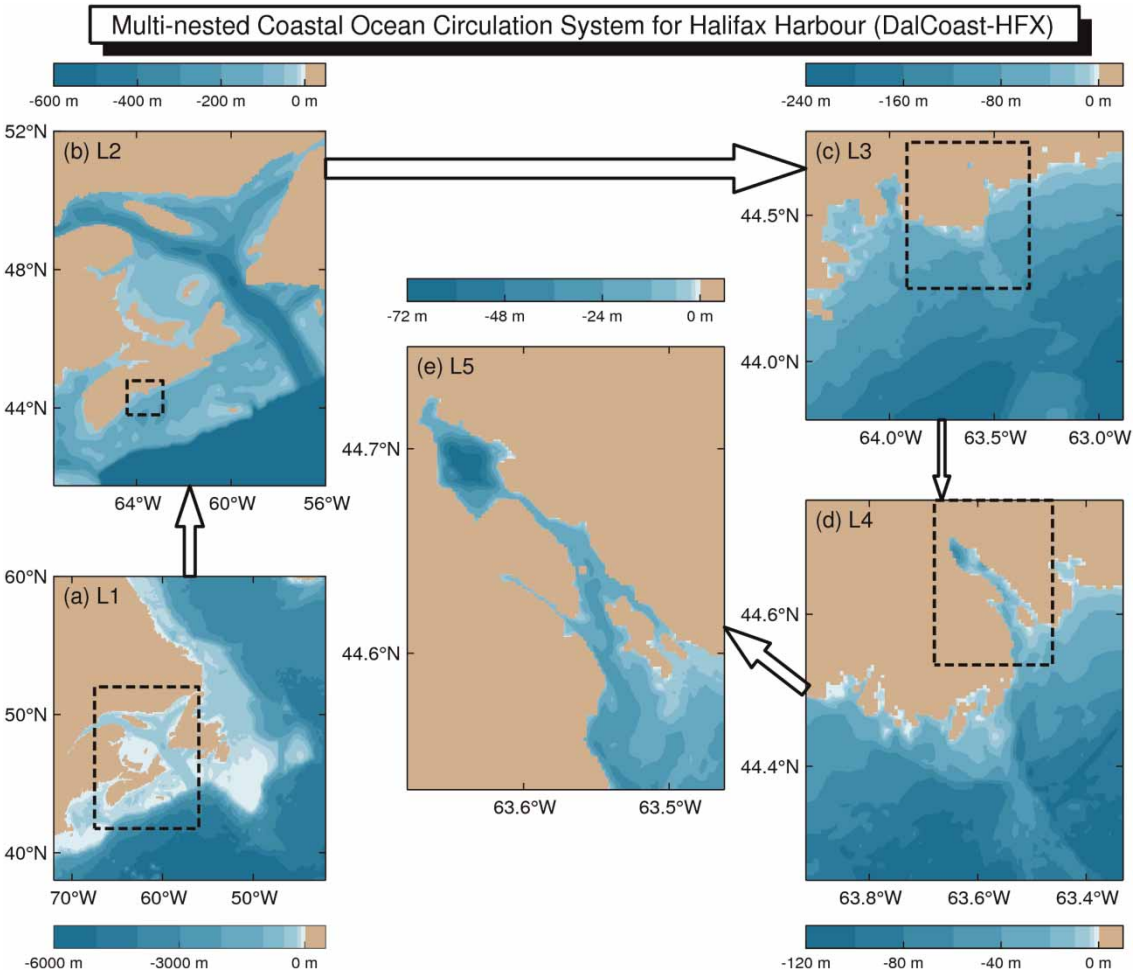

Figure 2 | Domains and major bathymetric features of the multi-nested ocean circulation modelling system. (a) Submodel L1 (horizontal resolution 1/12°, ~9 km) and (b) submodel L2 (1/16°, ~7 km) are DalCoast based on POM; (c) submodel L3 (~2 km), (d) submodel L4 (~500 m) and (e) submodel L5 (~200 m) are based on CANDIE. Land is marked by the tan colour. Please refer to the online version of this paper to see this figure in colour: http://www.iwaponline.com/wqrjc/toc.htm. With kind permission from Springer Science + Business Media: (Shan *et al.* (2011), Figure 8).

3D flow field is used in the passive tracer and particle tracking experiments.

Passive tracer and particle tracking

There are two general approaches for investigating the source, sink, pathway, dispersion and retention of substances of interest using a numerical model: the Eulerian and Lagrangian methods. In the Eulerian method, the evolution of a tracer concentration at any model grid point is calculated using the tracer equation. In the Lagrangian method, trajectories of particles are tracked based on model currents. Particle movement can be used to examine the source and sink of the substances, and quantify the hydrodynamic connectivity (Thompson *et al.* 2002; Sheng *et al.* 2009).

Passive tracer

The governing equation of the passive tracer is based on the following advection–diffusion equation:

$$\frac{\partial C}{\partial t}+\frac{\partial uC}{\partial x}+\frac{\partial vC}{\partial y}+\frac{\partial wC}{\partial z}=\frac{\partial}{\partial x}\left(A_{\mathrm{h}}\frac{\partial C}{\partial x}\right)+\frac{\partial}{\partial y}\left(A_{\mathrm{h}}\frac{\partial C}{\partial y}\right)+\frac{\partial}{\partial z}\left(A_{\mathrm{v}}\frac{\partial C}{\partial z}\right) \quad (1)$$

where C is the tracer concentration, (x, y, z, t) is space and time, (u, v, w) is the 3D flow field, and A_{h} and A_{v} are the

horizontal and vertical eddy diffusivity coefficients, respectively. In this study, A_h and A_v are calculated by the horizontal and vertical mixing schemes in the model. The model calculations of passive tracer concentrations are the same as those for temperature and salinity (active tracers), except that concentrations of passive tracers do not affect the model density and therefore have no effect on the flow dynamics. It should be noted that the CANDIE model uses fourth-order numerics and a flux limiter to calculate advection terms, which are very useful in accurately simulating (passive and active) tracer concentrations.

Flushing time is one of the important parameters in understanding and predicting the water quality level in coastal waters. We follow Sheng *et al.* (2009) and define the local flushing time as an e-folding time for the temporal decay of the volume averaged concentration (VAC) of each passive tracer. The VAC is defined as the volume integrated concentration of passive tracer concentrations over a specific subarea normalized by the total volume of the subarea. The temporal decay of VACs can be approximated by:

$$C = C_0 e^{-t/T_e} \tag{2}$$

where C is the VAC at time t, C_0 is the initial value of the VAC and equal to 1, and T_e is the e-folding flushing time.

Particle tracking

The movements of particles carried passively by the model currents are calculated using:

$$\vec{x}^{t+\Delta t} = \vec{x}^{t} + \int_{t}^{t+\Delta t} \vec{u}(\vec{x}, t)\mathrm{d}t + \vec{\delta} \tag{3}$$

where $\vec{x}^{t+\Delta t}$ and $\vec{x}^{t}$ are 3D position vectors of a passive particle at time $t+\Delta t$ and previous time t, respectively. Here, $\vec{u}(\vec{x}, t)$ is the 3D velocity vector of model currents, and $\vec{\delta}$ is a random walk process to account for particle movement associated with subgrid scale turbulence and other local processes that are not resolved by the model. We follow Taylor (1922) and express $\vec{\delta}(\delta x, \delta y, \delta z)$ as:

$$\delta x = \xi\sqrt{2K_x\Delta t}, \quad \delta y = \xi\sqrt{2K_y\Delta t}, \quad \delta z = \xi\sqrt{2K_z\Delta t} \tag{4}$$

where ξ is a Gaussian random, K_x, K_y and K_z are eddy diffusivity coefficients for the random walk in the x, y and z directions, and Δt (30 min) is the time step used in the integration of (3). Based on the field dye tracing experiments and movements of surface drifters, the observed horizontal and vertical eddy diffusivity coefficients in coastal waters range from 0.1 to $10\,\mathrm{m^2\,s^{-1}}$ and from 0.1×10^{-3} to $10\times10^{-3}\,\mathrm{m^2\,s^{-1}}$, respectively (Riddle & Lewis 2000; Tseng 2002; Thompson *et al.* 2002). In this study, we set the horizontal diffusivity (K_h) of the random walk to be homogeneous and isotropic ($K_x = K_y = K_h$) with a characteristic value of $1\,\mathrm{m^2\,s^{-1}}$ ($K_h = 1\,\mathrm{m^2\,s^{-1}}$), and set the vertical diffusivity to be 10^3 times smaller than the horizontal diffusivity ($K_z = 1\times10^{-3}\,\mathrm{m^2\,s^{-1}}$). A sensitivity study of low ($K_h = 0.1\,\mathrm{m^2\,s^{-1}}$, $K_z = 0.1\times10^{-3}\,\mathrm{m^2\,s^{-1}}$) and high ($K_h = 10\,\mathrm{m^2\,s^{-1}}$, $K_z = 10\times10^{-3}\,\mathrm{m^2\,s^{-1}}$) eddy diffusivity coefficients is also considered in this study to address the role of the eddy diffusivity in dispersing particles in the Harbour. The fourth-order Runge–Kutta scheme (Press *et al.* 1992) is used to track the passive particles. Based on the trajectories of particles, the connectivity matrix can be calculated to quantify the hydrodynamic connectivity among different areas (Thompson *et al.* 2002).

MODEL RESULTS

Circulation and validation

Circulation in Halifax Harbour is affected by tides, wind forcing and freshwater discharge. Shan *et al.* (2011) recently investigated the 3D circulation and hydrography in the Harbour under normal conditions. In this study, we examine the circulation in the Harbour during storms based on model results. This is of particular importance because the high volume sewage discharge usually occurs during storm events. Storm surge and storm-induced currents play a vital role in affecting the dispersion and retention in Halifax Harbour, particularly

during the late summer, autumn and winter. Two storms in 2006 (labelled as storms A and B) are selected in this paper. Storm A swept over the Scotian Shelf and adjacent waters on 1 February 2006 (Figure 3), with the storm track on the eastern side of Halifax Harbour. Storm B passed over Halifax Harbour 18 days later, with its storm track on the western side of the Harbour (Figure 3). The wind direction in Halifax Harbour changed in an anti-clockwise direction during storm A, and in a clockwise direction during storm B. We will demonstrate that the relative position between the storm centre and Halifax Harbour can cause significant differences in circulation, flushing time and dispersion in the Harbour during these two storm events.

Figures 4 and 5 present near-surface currents and salinity produced by submodel L5 during the two storms, which demonstrate that the near-surface currents in Halifax Harbour are significantly affected by the winter storms. At the peak of storm A (Figure 4(c)), the wind is from the north, and an intense storm-induced coastal

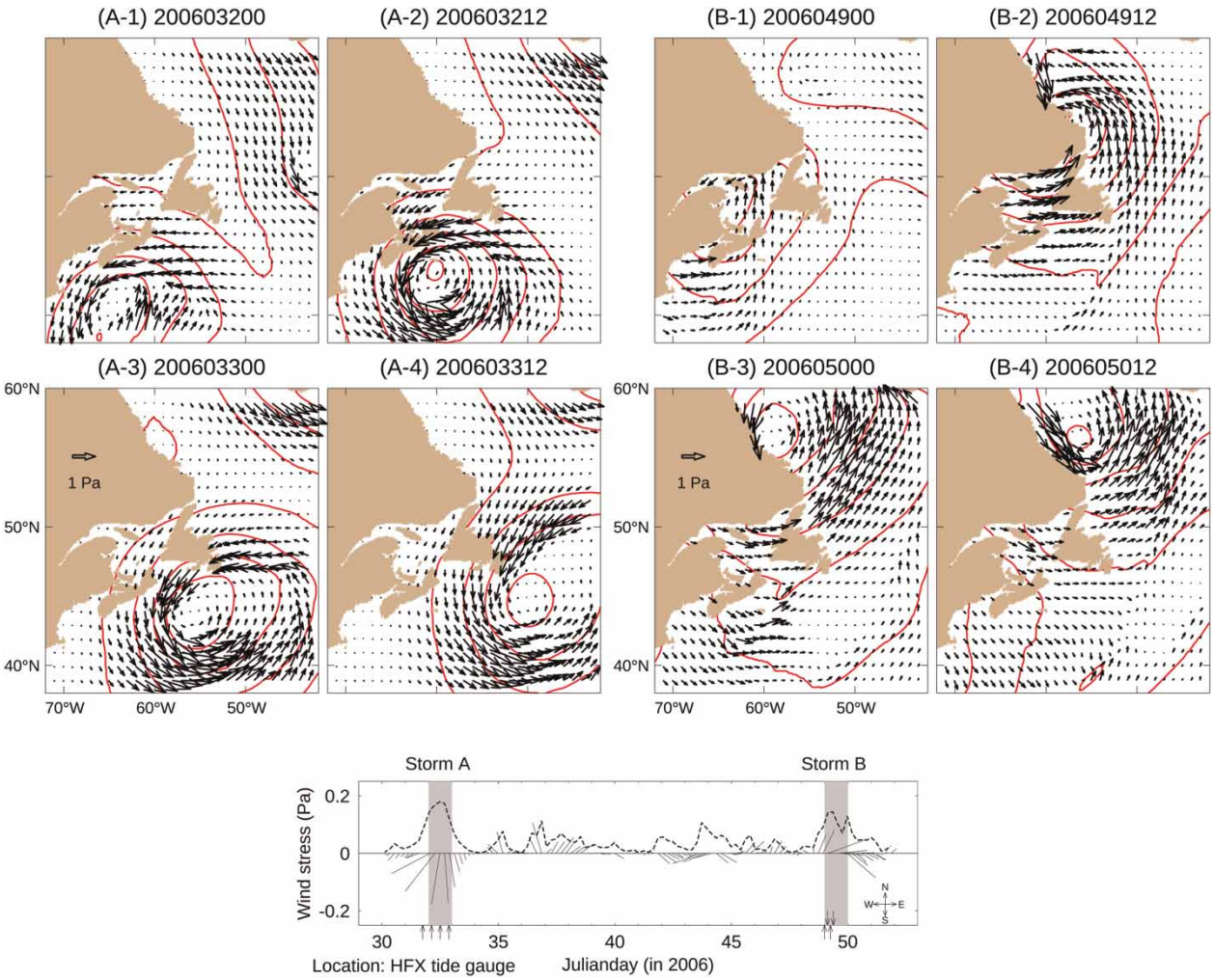

Figure 3 | Wind stress (black arrows) and atmospheric pressure at sea level (red contour lines) over the eastern Canadian shelf during winter storms A and B, taken from 3 hourly numerical weather forecasts produced by the Meteorological Service of Canada. Storm A: (A-1) 00:00 1 February, (A-2) 12:00 1 February, (A-3) 00:00 2 February and (A-4) 12:00 UTC 2 February 2006. Storm B: (B-1) 00:00 18 February, (B-2) 12:00 18 February, (B-3) 00:00 19 February and (B-4) 12:00 UTC 19 February 2006. Bottom panel shows time series of wind forcing at HFX tide gauge (Figure 1) for February 2006. The dashed line represents the wind stress amplitude. The grey shaded areas indicate two winter storm events. The vertical arrows point out the time frames during the storms, which are used in the detailed discussion. Please refer to the online version of this paper to see this figure in colour: http://www.iwaponline.com/wqrjc/toc.htm.

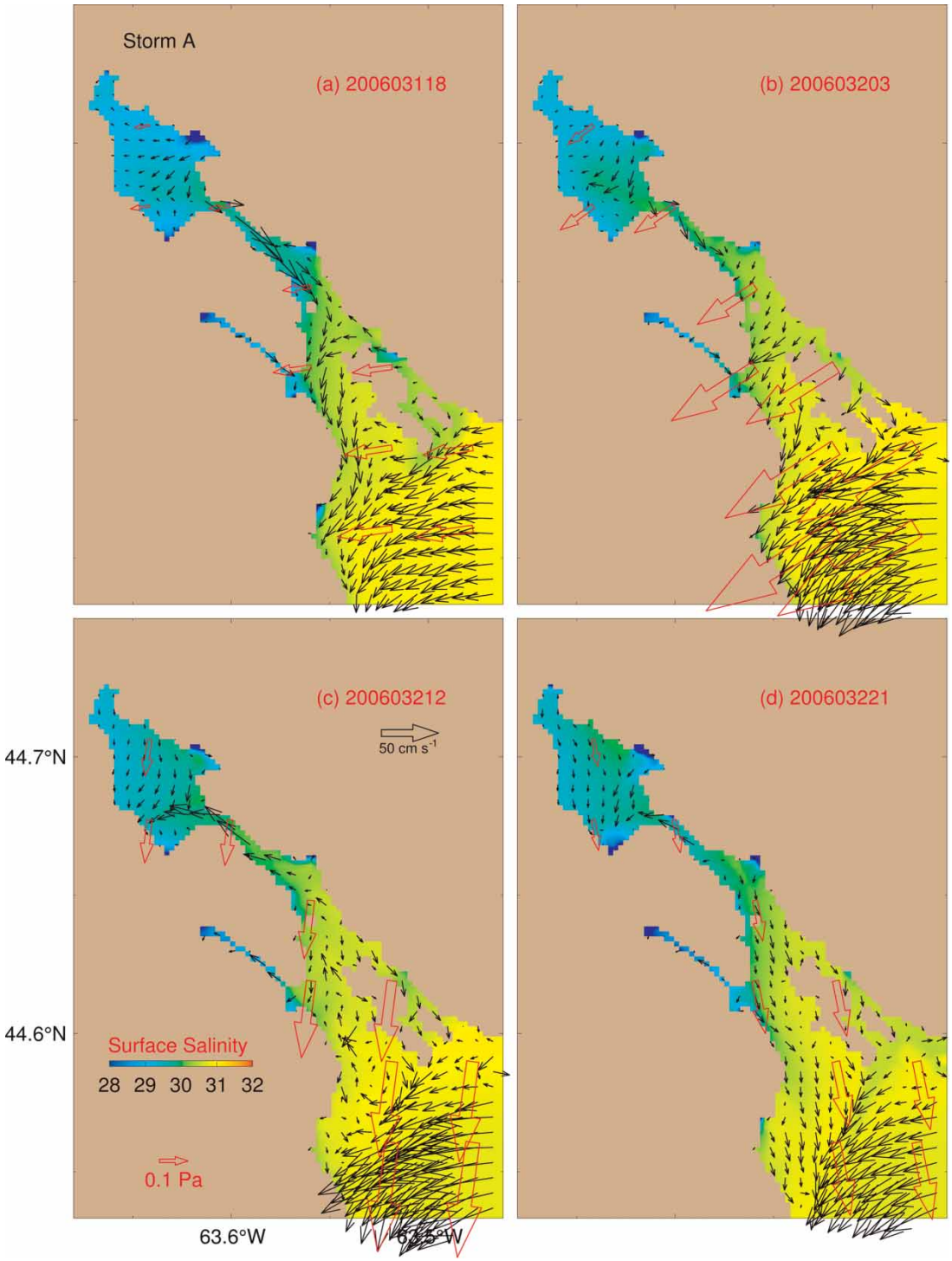

Figure 4 | Near-surface (2 m) currents and salinities produced by submodel L5 during winter storm A at (a) 18:00 31 January, (b) 03:00 1 February, (c) 12:00 1 February and (d) 21:00 1 February 2006. Red open arrows are wind stress vectors. For clarity, velocity vectors are plotted at every third model grid point. Please refer to the online version of this paper to see this figure in colour: http://www.iwaponline.com/wqrjc/toc.htm.

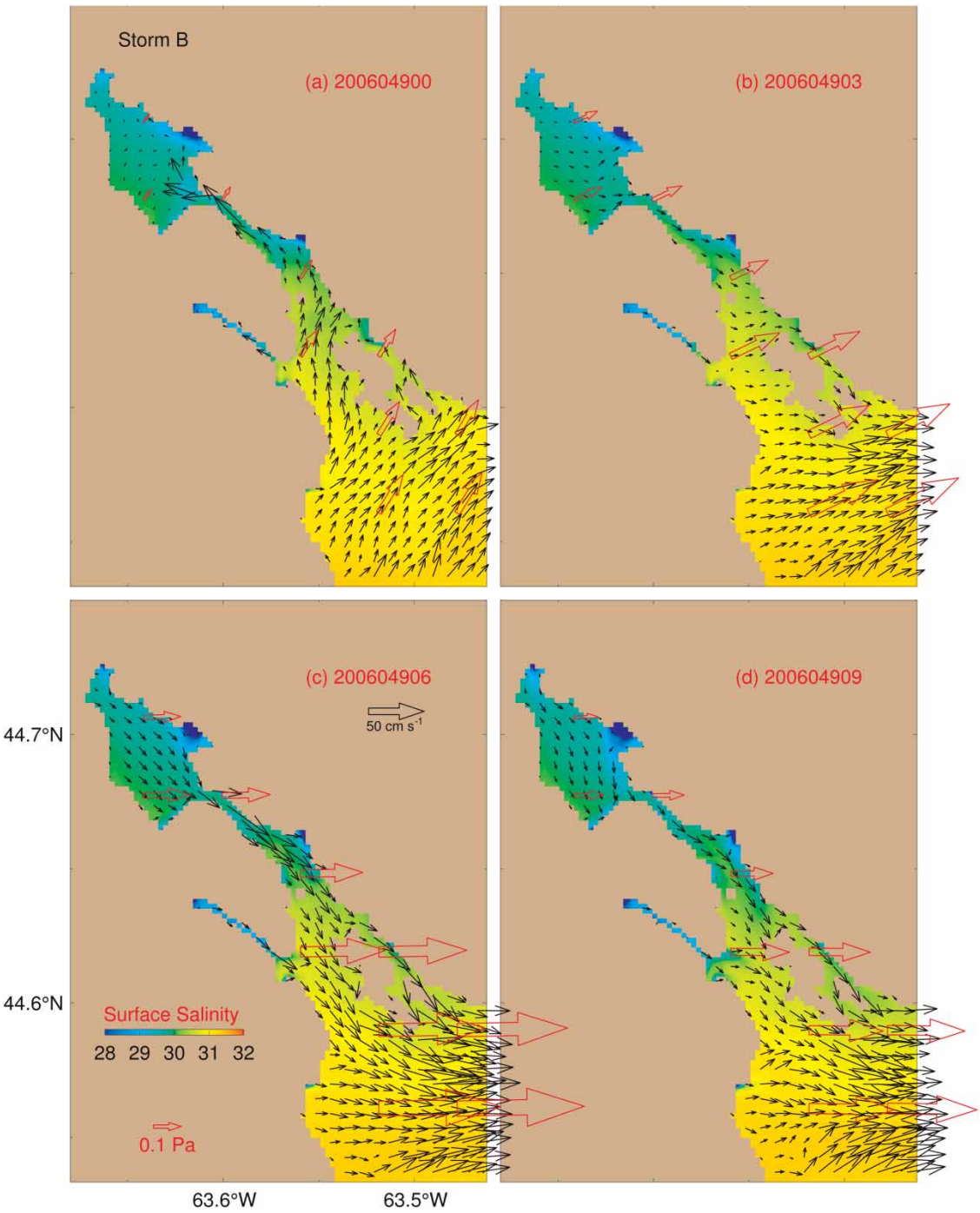

Figure 5 | Near-surface (2 m) currents and salinities produced by submodel L5 during winter storm B at (a) 00:00 18 February, (b) 03:00 18 February, (c) 00:06 18 February and (d) 00:09 18 February 2006.

current produced by submodel L4 extends to the Outer Harbour. The flood tidal current can be seen in the Narrows, indicating the strong tidal effect over this region. At the peak of storm B (Figure 5(c)), the wind direction is from the west, and the flow in the Harbour is almost uniform and southeastward due to the combined result of the ebb tide and local offshore wind forcing.

The hydrodynamic response of the Harbour to tides, wind stress and buoyancy forcing, and the performance of the multi-nested modelling system were presented in Shan *et al*. (2011). In the following discussion, we only assess the skill of submodel L5 in simulating sea surface elevations, tidal currents, temperature and salinity, and baroclinic flow in the Harbour.

Sea level

Sea level observations have been made in Halifax Harbour for almost a century. At the present time, there are two tide gauges in the Harbour, one near the Naval Dockyard and the other near the Bedford Institute of Oceanography (BIO) (Figure 1). Figure 6 presents time series of observed and simulated sea level at the two tide gauges for the first 3 months of 2006. The tides in Halifax Harbour are predominantly semi-diurnal. A pronounced spring and neap variation is also evident, due mainly to the interaction of the M_2 and S_2 tidal constituents. The non-tidal component of the total sea level during storm A is significantly higher than the value during storm B, due to the fact that large storm-induced surge waves were excited by storm A.

A performance index, γ^2 (Thompson & Sheng 1997), is used to quantify the skill of submodel L5 in simulating the tidal and non-tidal sea level variations in the Harbour:

$$\gamma^2 = \frac{\mathrm{Var}(O - M)}{\mathrm{Var}(O)} \tag{5}$$

where Var represents the variance, and O and M denote the observed and simulated variables, respectively. The smaller the value of γ^2 is, the better the performance of submodel L5 has. Empirically, the threshold value of γ^2 is chosen to be 1. The γ^2 values are less than 0.03 for tides and 0.3 for non-tidal components for both tide gauges during this 3 month period, indicating that submodel L5 performs well in reconstructing the sea level variations in Halifax Harbour.

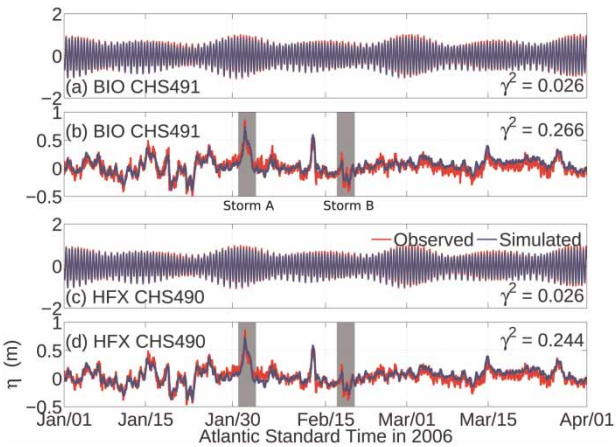

Figure 6 | Tidal and non-tidal sea surface elevations (η) at two Canadian Hydrographic Service (CHS) tide gauges (a), (b) CHS491 and (c), (d) CHS490 for January, February and March 2006. Observed values are in red and simulated in blue. The simulated results are produced by submodel L5. The observed and simulated sea surface elevations are separated into tidal (a), (c) and non-tidal (b), (d) components using T_TIDE MATLAB package (Pawlowicz *et al*. 2002). The grey shaded vertical bars indicate two storm events in February 2006. Please refer to the online version of this paper to see this figure in colour: http://www.iwaponline.com/wqrjc/toc.htm.

Tidal current

There were no current observations in the Harbour during the study period. We assess the performance of submodel L5 in simulating tidal circulation by comparing the tidal currents produced by submodel L5 with the depth-averaged tidal currents produced by WebTide. WebTide is a computer program designed to provide tidal elevations and depth-averaged tidal currents for a given area based on pre-calculated tidal harmonics. In this study, the WebTide dataset for Halifax Harbour (Greenberg 1999) is used. Since the month-to-month variability of depth-averaged tidal currents in Halifax Harbour produced by submodel L5 are small, we examine only the simulated depth-averaged M_2 tidal current ellipses in March 2006, during which the upper water column is relatively well mixed.

The depth-averaged M_2 tidal currents in March 2006 produced by submodel L5 are relatively weak in Bedford Basin and relatively strong in the Narrows (blue ellipses in Figure 7; please refer to the online version of this paper to see this figure in colour: http://www.iwaponline.com/wqrjc/toc.htm). The simulated M_2 tidal current ellipses in the Narrows are nearly rectilinear. Circular-shaped tidal current ellipses occur over areas to the southeast of Lawlor Island. The four parameters of each M_2 tidal current ellipse including the semi-major axis, eccentricity, inclination and phase calculated from currents produced by submodel L5 agree reasonably well with the Halifax Harbour WebTide (Figure 7). The differences of M_2 tidal current ellipses between our model results and WebTide can be attributed to the use of different open boundary conditions. In DalCoast-HFX, sea

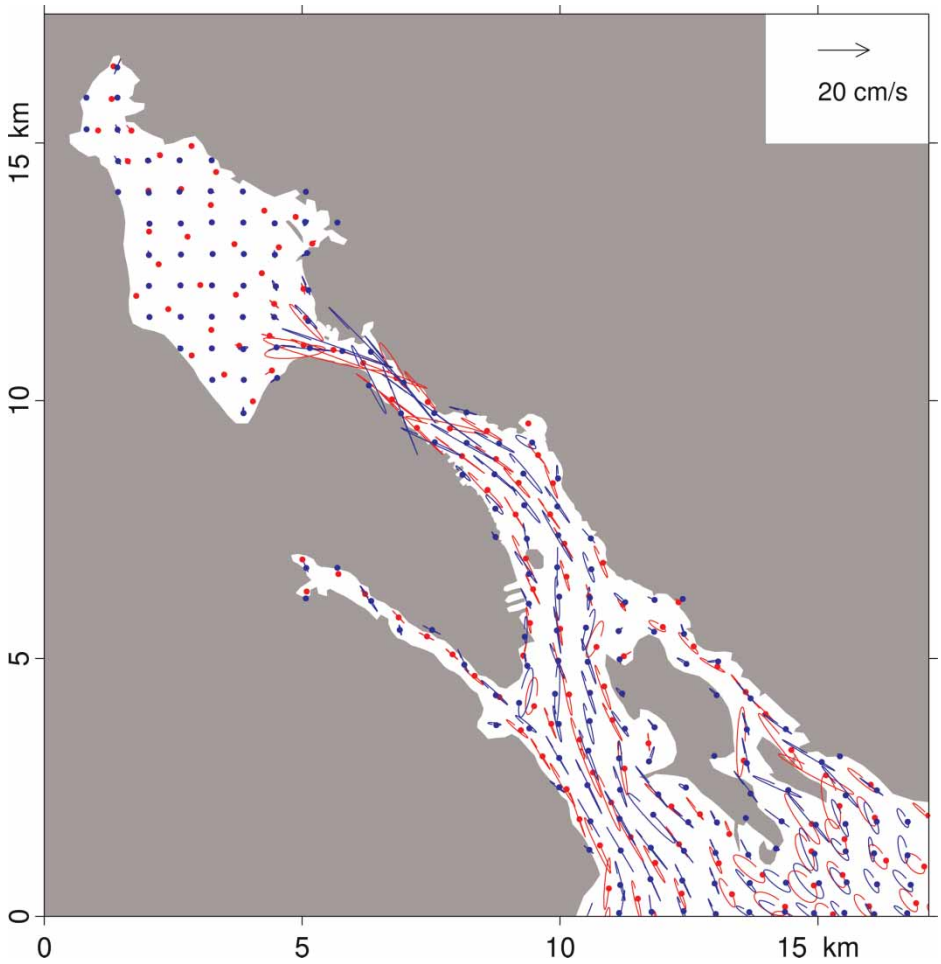

Figure 7 | Comparison of depth-averaged M_2 tidal current ellipses from submodel L5 (blue, at every third model gird point) and WebTide for Halifax Harbour (red, for clarity, the minimum distance between points is 600 m). Please refer to the online version of this paper to see this figure in colour: http://www.iwaponline.com/wqrjc/toc.htm.

surface elevations and depth-averaged currents are specified at the open boundary of submodel L2. The tidal signals propagate to the domain of submodel L5 using the one-way nesting technique. In comparison, a simple tidal boundary condition was used in the single-domain tidal model for generating the WebTide dataset of Halifax Harbour (Greenberg 1999).

Temperature and salinity profiles

Observations were made in 2006 through the Halifax Harbour Water Quality Monitoring Program, including temperature and salinity profiles. Figure 8 presents simulated and observed temperature and salinity profiles at station G2 in Bedford Basin and station B2 in the Outer Harbour (Figure 1). For comparison, the vertical profiles of monthly mean climatology (Shan *et al.* 2011) are also shown in the figure. Submodel L5 has reasonable skill in simulating the vertical distributions and associated variabilities of temperature and salinity in Halifax Harbour. In the top 20 m of the two stations, the simulated monthly mean temperature and salinity profiles are in the range of corresponding observations made in 2006. In Bedford Basin, the simulated temperature and salinity profiles exhibit the seasonal development of thermocline due mainly to heat fluxes at the surface and freshwater plume due to the water discharge from Sackville River, which are in good agreement with the observations. In the Outer Harbour, the simulated temperature and salinity profiles are relatively well mixed throughout the year, except for a weak stratification in summer due to the energetic environment in the open ocean and shallow water depth ($\sim$20 m) at the site, which are also

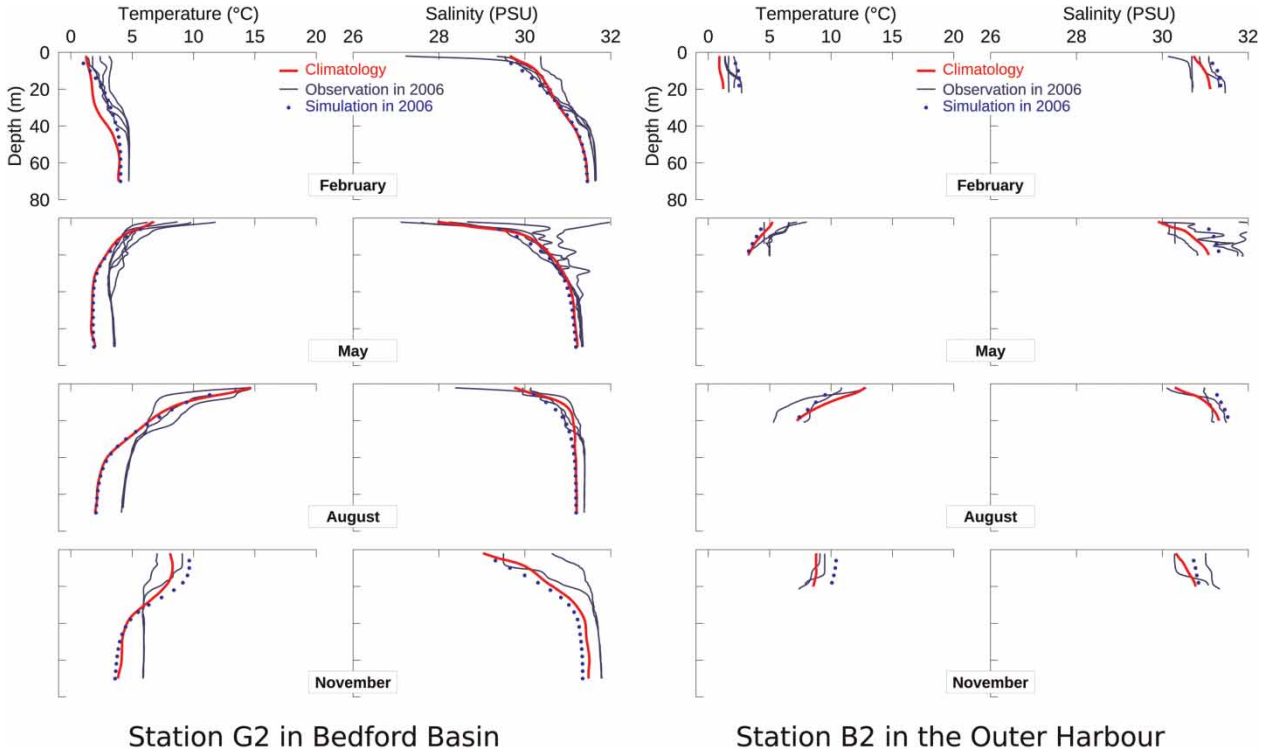

Figure 8 | Vertical profiles of observed (blue solid) and simulated (blue dotted) monthly mean temperature and salinity (in the practical salinity unit, PSU) at station G2 in Bedford Basin and station B2 in the Outer Harbour. The monthly mean climatologies of the temperature and salinity (red) at the two stations are also shown. Please refer to the online version of this paper to see this figure in colour: http://www.iwaponline.com/wqrjc/toc.htm.

in good agreement with the observations. In the lower water column of Bedford Basin, however, the simulated temperature is cooler and the simulated salinity is fresher than the observed values. It should be noted that the simulated temperature and salinity in Bedford Basin, particularly in the lower water column agree well with the monthly mean climatology, which is due to the use of the spectral nudging method (Thompson *et al.* 2007) in the model. A non-hydrostatic model with high horizontal and vertical model resolution, spatially varying mixing parameterization over the Narrows and Bedford Basin is needed in order to further improve the performance of the submodel L5 in simulating the intra- and inter-annual variabilities of temperature and salinity in Halifax Harbour, especially in Bedford Basin.

Two-layer estuarine circulation

The simulated annual mean temperature in Halifax Harbour is relatively uniform in the top 30 m from Bedford Basin to the Outer Harbour (Figure 9), with a cold water pool in the deep layer of Bedford Basin. In comparison, the simulated annual mean salinity in the Harbour has significant horizontal and vertical variations (Figure 9). Three distinct water masses are identified: the fresher water in the top layer of Bedford Basin due to the water discharge from the Sackville River; the salty shelf water intruded from the entrance of the Harbour; and the salty water in the bottom layer of Bedford Basin. The simulated annual mean horizontal circulation is shown in the bottom panel of Figure 9 and features a typical two-layer estuarine circulation with seaward flow in the upper layer, and landward return flow in the lower layer. The annual mean currents are relatively weak in Bedford Basin, and relatively strong in the Narrows and the Inner and Outer Harbour.

Flushing time

To quantify the flushing time and associated spatial variability, five different passive tracers are initialized over five different subareas in Halifax Harbour. These five subareas are: (1) the entire Bedford Basin (tracer 1), (2) the upper 20 m layer in

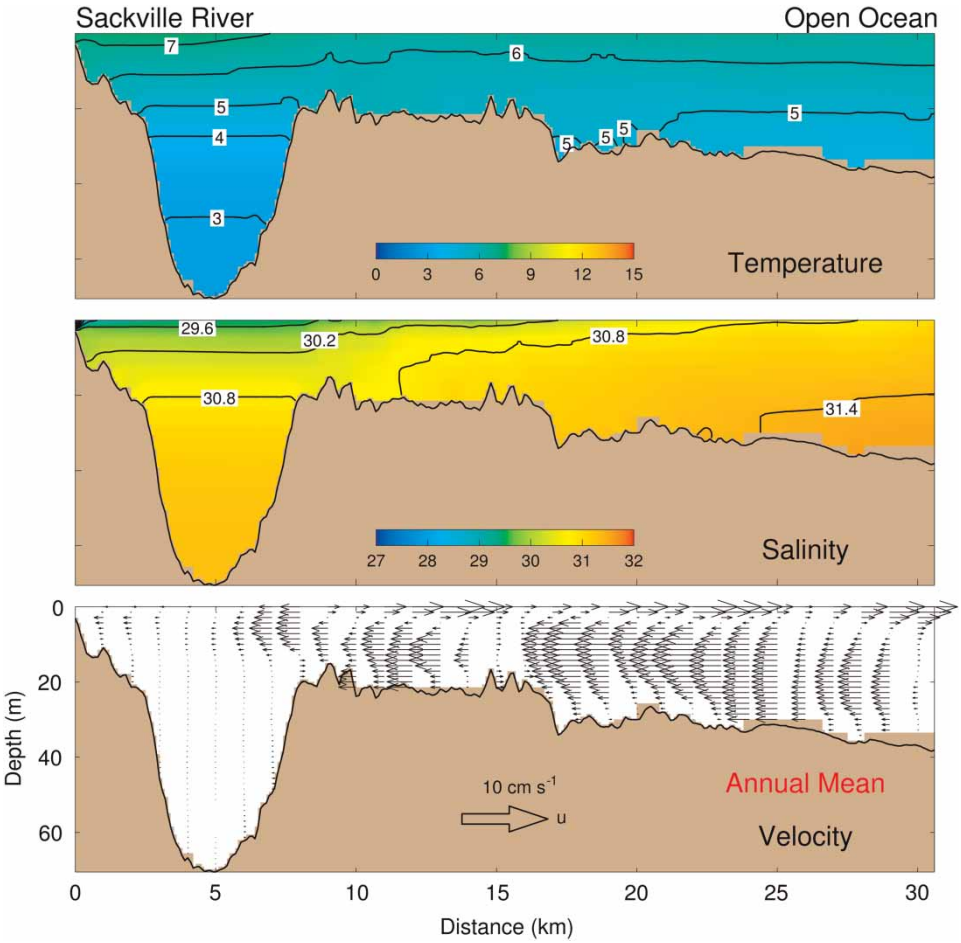

Figure 9 | Transect view of annual mean temperature, salinity and horizontal current from the Sackville River to the open ocean in Halifax Harbour (see red dashed line in Figure 1) calculated from results produced by submodel L5.

Bedford Basin (tracer 2), (3) the Narrows (tracer 3), (4) the Inner Harbour (tracer 4) and (5) the Outer Harbour (tracer 5). The initial concentration of each tracer is set to one within the specific subarea and zero outside the given subarea. Figure 10(a) shows the initial distribution of concentrations for tracer 1 along the transect from the head of Sackville River to the open sea (red dashed line in Figure 1; please refer to the online version of this paper to see this figure in colour: http://www.iwaponline.com/wqrjc/toc.htm). In order to examine seasonal variations of tracer concentrations and flushing time over the five subareas defined above, concentrations of the five tracers are reinitialized on the first day of January, April, July and October in 2006, respectively, and calculated with other model variables in the multi-nested modelling system.

Figures 10 and 11 present concentration distributions along the transect at days 0, 10, 20 and 30 for tracers 1 and 2 after the initial release on 1 January 2006 in the entire and the upper Bedford Basin, respectively. Figures 10(b) and 10(c) show a very thin layer near the sea surface with relatively high concentrations of tracer 1 spreading seaward in the Narrows at day 10 and 20, respectively. In Bedford Basin, a sub-surface layer at a depth of about 5 m, with relatively low concentrations of tracer 1, forms from the Narrows to the head of Bedford Basin (Figures 10(b) and 10(c)). After 30 days, the concentrations of tracer 1 in the lower layer of Bedford Basin (Figure 10(d)) decrease slowly with time. The tracer dispersion in the upper Bedford Basin is relatively fast and affected by the strong tidal currents and wind-induced mixing, while the tracer dispersion in the lower layer of Bedford Basin is relatively slow and affected mainly by diffusion. In comparison, concentrations of tracer 2 are dispersed to the open sea via

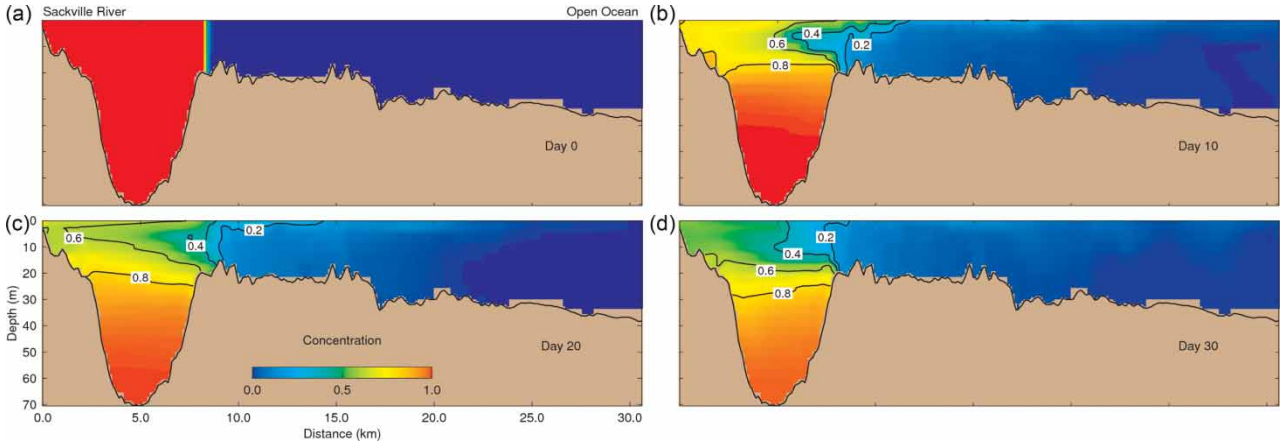

Figure 10 | Vertical distributions of concentrations for passive tracer 1 (entire Bedford Basin) along the transect (Figure 1) on (a) 1 January, (b) 11 January, (c) 21 January and (d) 31 January 2006. The initial tracer concentration is set to unity in the entire Bedford Basin and zero elsewhere on 1 January 2006.

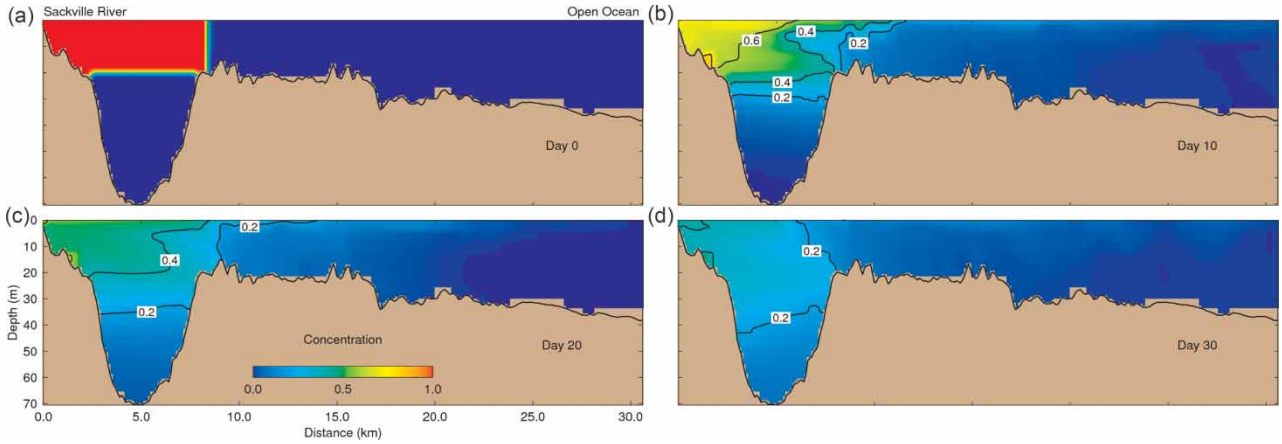

Figure 11 | Same as Figure 10, except for tracer 2 (upper Bedford Basin), where the initial concentration is set to unity in the upper Bedford Basin and zero elsewhere on 1 January 2006.

the Narrows and also diffused to the lower layer of Bedford Basin (Figure 11). The concentrations of tracer 2 at day 30 are reduced from unity to about 0.3 in the upper Bedford Basin (Figure 11(d)).

Based on the time-varying 3D tracer concentrations produced by the model, the VACs are calculated and presented in Figure 12 for each subarea in the four seasons. Figure 12(a) shows time series of the VACs during the 90 day period for tracer 1 over the entire Bedford Basin. The VACs of tracer 1 decrease exponentially with time due to the transport and dispersion of the passive tracer from Bedford Basin to the other areas of the Harbour. The four curves in Figure 12(a) represent VACs in the four different seasons in 2006. The VACs of tracer 1 decay faster in winter than in the other three seasons, due mainly to the strong westerly or northwesterly winds in winter that enhance the two-layer estuarine circulation and mixing in the upper water column. Figure 12(a) also shows the high-frequency variability of the VACs, with a typical period of about 12 hours, which is due mainly to the tracer patch flowing in and out of Bedford Basin caused by tides. Based on the time series of VACs in the four seasons as shown in Figure 12(a) and Equation (2), the estimated e-folding flushing time for the entire Bedford Basin is about 90.6 days.

The time series of VACs for tracer 2 (of which the initial concentration is set to 1 in the upper 20 m of Bedford Basin) show a relatively faster decay (Figure 12(b)) in comparison

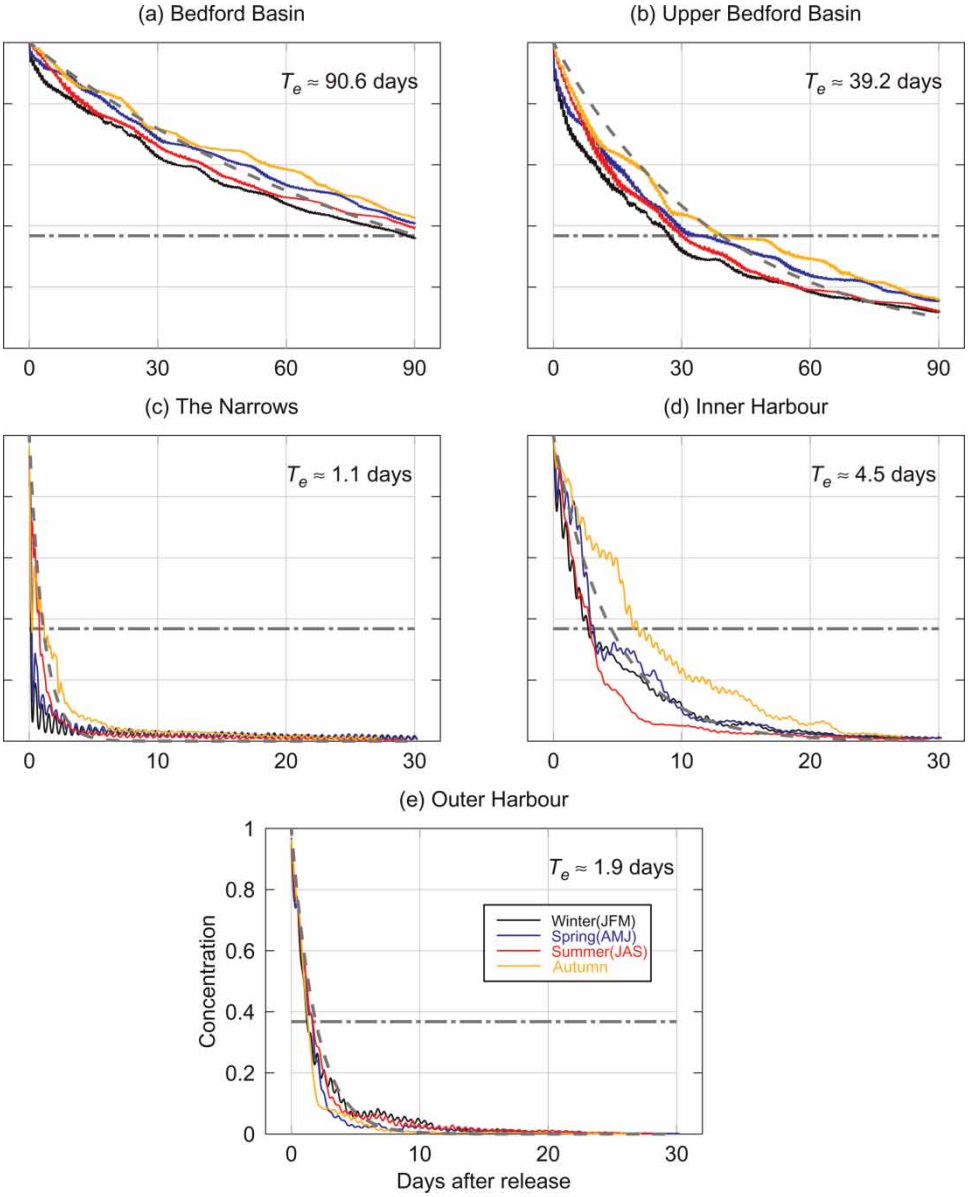

Figure 12 | Time series of volume averaged concentrations (VACs) of passive tracers for five different subareas in Halifax Harbour for all four seasons in 2006.

with the results for tracer 1. The estimated e-folding flushing time of the upper Bedford Basin is about 39.2 days. Figures 12(c)–12(e) demonstrate the fast temporal decay of VACs in the Narrows, Inner and Outer Harbour, with estimated e-folding flushing times at about 1.1, 4.5 and 1.9 days, respectively. The estimated e-folding flushing time of the Narrows is the shortest among the five subareas due to strong dispersion associated with the intense tidal currents in the area.

An additional tracer experiment was conducted to identify which areas in the Harbour will be likely to accumulate sewage pollutants. The tracer concentrations in this new experiment are set to unity near sewage outfalls at each model time step, with the initial concentration set to zero in the entire Harbour on 1 January 2006. Figure 13 presents the distributions of near-surface tracer concentrations in Halifax Harbour at the end of days 10, 100, 200 and 365 in 2006. After 100 days, the tracer concentration in Halifax

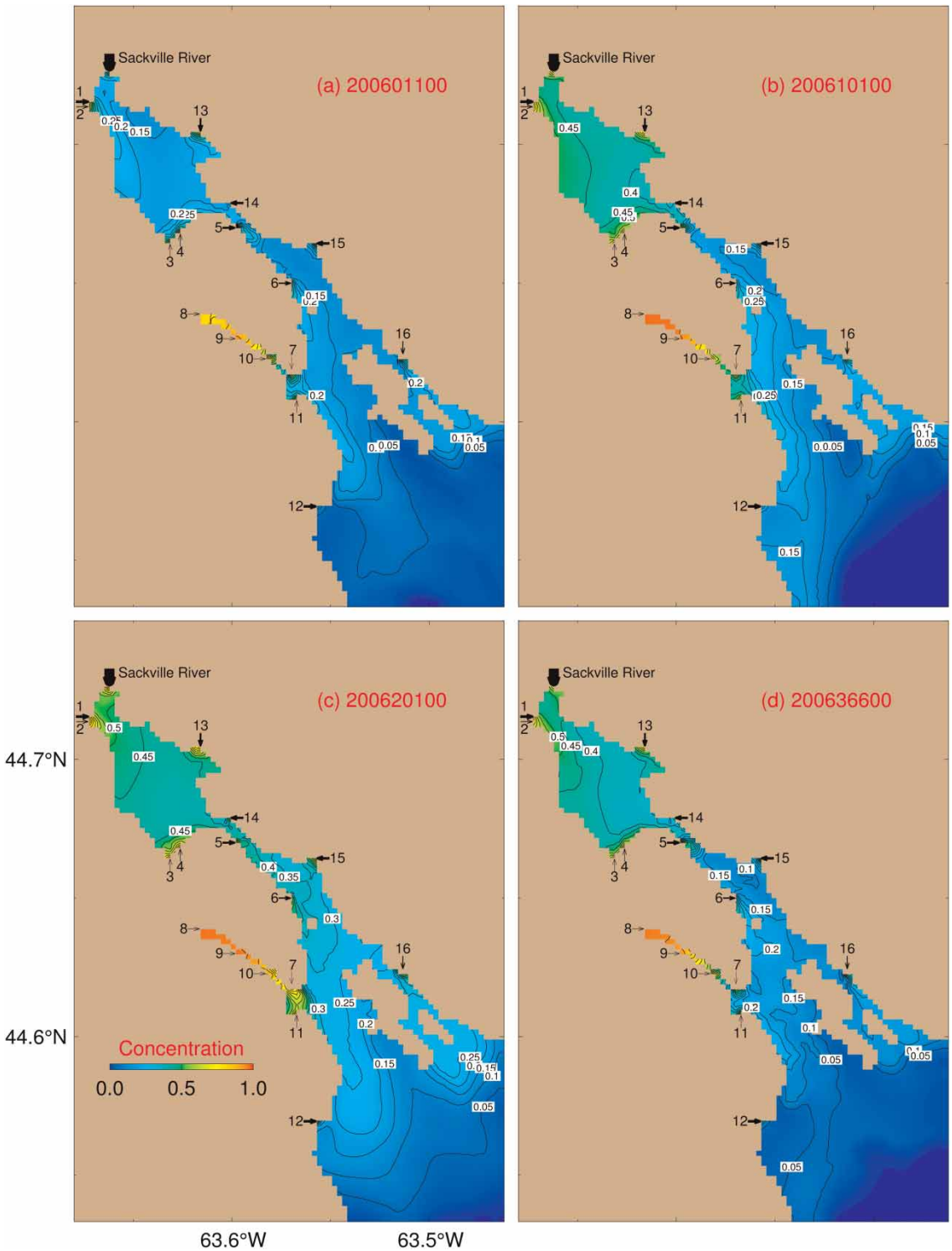

Figure 13 | Tracer concentrations at the top *z*-level (centred at 2 m) at the end of days (a) 10, (b) 100, (c) 200 and (d) 365 in 2006. The tracer concentrations at water discharge outfalls are set to unity at each time step. Water discharge locations are numbered 1 to 16 and discharge values are indicated by scaled arrows.

Harbour reaches a quasi-steady state statistically, which is characterized by relatively higher tracer concentrations over the Northwest Arm, Bedford Basin and local areas near the sewage outfalls. The tracer concentrations over the Narrows, Inner and Outer Harbour vary periodically due to the flood and ebb tide, and storm events. At the end of 2006, the tracer concentrations are about 0.45, above 0.5, 0.2, below 0.15 in Bedford Basin, the Northwest Arm, Narrows and Inner Harbour, and Outer Harbour, respectively.

Dispersion and retention

As mentioned earlier, movements of passive particles are affected by currents and eddy diffusivity coefficients (K_h and K_z) for the random walk process that are not resolved by the model. Nine particle tracking experiments (Table 1) were conducted using the 3D annual mean (time-independent) and instantaneous flow fields during storm events (see Figures 4, 5 and 9) in 2006 produced by sub-model L5, with different values of K_h and K_z. The passive particles are released in the top z-level (Figure 14). The initial separation distance between two adjacent particles is set to 100 m.

In experiment M-m (Table 1), in which the annual mean model currents and moderate diffusivity coefficients are used, particles are tracked for 5 days, and the results are presented in Figure 15. Most particles released in the near-surface of Bedford Basin and the Northwest Arm in this experiment are retained within the areas with gradual seaward spreading due mainly to weak near-surface currents (Figure 15). In the Narrows, Inner and Outer Harbour, only a small percentage of particles remain in the near-surface layer, with most of the particles scattering along the deep channel in the Harbour, indicating that most of the particles in the near-surface layer move seaward (southeastward) and exit from the open boundary of submodel L5. There are a significant number of particles transported from the near-surface layer to the sub-surface layer (Figure 15), indicating that the model vertical velocity component plays an important role in advecting passive particles in the Harbour. In the sub-surface layer, the particles drift landward (northwestward) associated with the landward currents.

To examine the effects of tides, wind and freshwater discharge on the movements of passive particles in Halifax Harbour, the results using the moderate diffusivity coefficients and instantaneous model currents during storm A

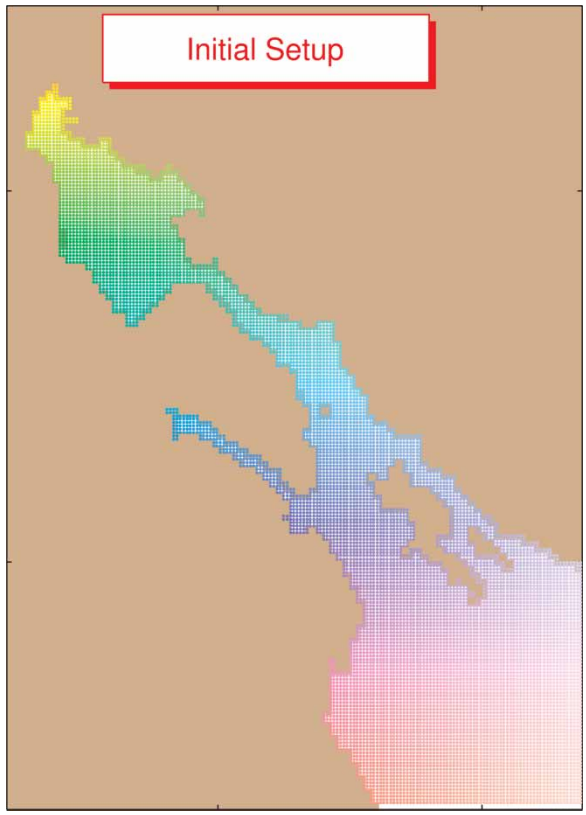

Figure 14 | Initial positions of colour-coded particles released in the top z-level (centred at 2 m) in Halifax Harbour. The initial separation distance between two adjacent particles is set to 100 m. Please refer to the online version of this paper to see this figure in colour: http://www.iwaponline.com/wqrjc/toc.htm.

Table 1 | List of nine particle tracking experiments using different model currents and different (low, moderate and high) values of the horizontal diffusivity coefficient for the random walk process. The vertical diffusivity coefficient K_z in the nine experiments is set to 10^{-3} K_h

Experiment	Flow field	Random walk ($m^2 s^{-1}$) K_h
M-m	Annual mean	1.0
A-m	Instantaneous during storm A	
B-m	Instantaneous during storm B	
M-l	Annual mean	0.1
A-l	Instantaneous during storm A	
B-l	Instantaneous during storm B	
M-h	Annual mean	10.0
A-h	Instantaneous during storm A	
B-h	Instantaneous during storm B	

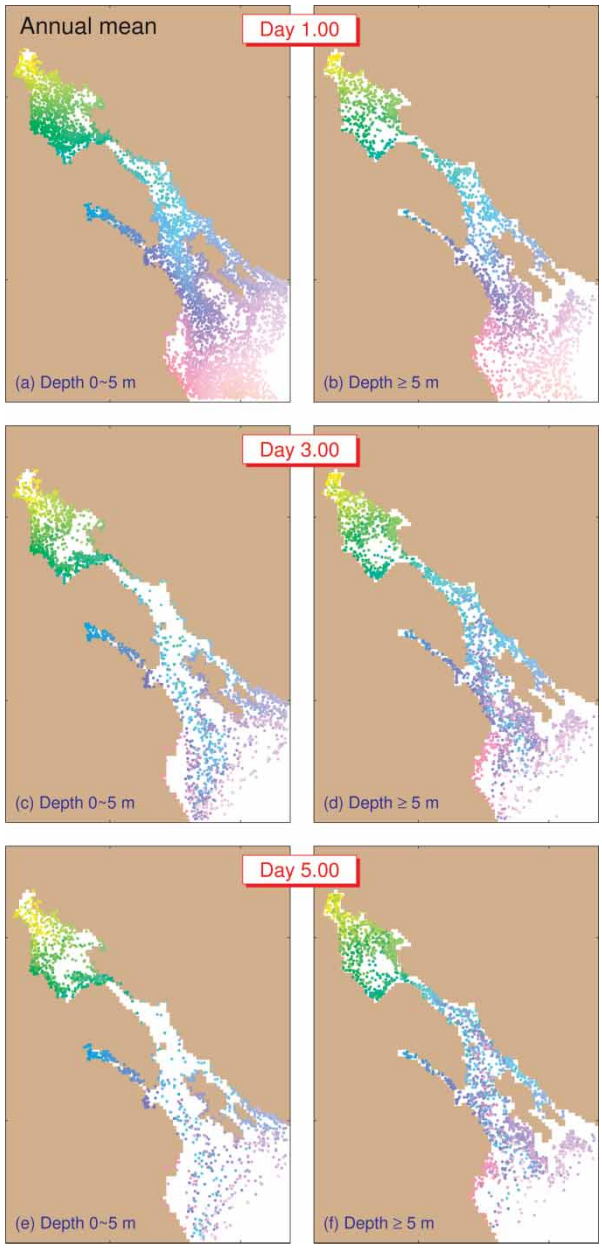

Figure 15 | Distributions of particles in the near-surface layer (0 ~ 5 m) and the sub-surface layer (≥5 m) 1 day (top panel), 3 days (middle panel) and 5 days (bottom panel) after the initial release in the near-surface layer in Halifax Harbour. The 3D annual mean currents produced by submodel L5 with moderate diffusivity coefficients (M-m, Table 1) were used in the particle tracking.

(experiment A-m) and storm B (B-m) are presented in Figures 16 and 17. The initial positions of passive particles are the same as in experiment M-m (Figure 14). Particles are released in the top z-level at the beginning of each day and carried passively by time-dependent 3D currents produced by submodel L5. The major difference in wind forcing between these two days, as mentioned earlier, is that the wind direction in Halifax Harbour changes in an anti-clockwise direction during storm A, and in a clockwise direction during storm B (Figure 3). This is because storm A's track is on the eastern side of Halifax Harbour, and storm B's track is on the western side (Figure 3). It is also worthwhile to note that tides in the Harbour are in the flood phase at the beginning of day 32, and in the ebb phase at the beginning of day 49. For particles released during storm A (experiment A-m), a large amount of near-surface particles gather along the western side of Halifax Harbour from the Sackville River to the open sea (Figures 16(a) and 16(c)) due mainly to the strong storm-induced near-surface currents. Some of the particles are carried from the near-surface layer to the sub-surface layer, with most of the particles gathering along the coastline in the Harbour (Figures 16(b) and 16(d)). For particles released during storm B (experiment B-m), most of the particles in the near-surface drift seaward (Figures 17(a) and 17(c)). The near-surface particles in Bedford Basin are converged to the southeastern part of the Basin and moved into the Narrows. A large amount of near-surface particles drift along McNabs Island and exit from the open boundary of submodel L5 (Figure 17(c)), due mainly to the storm-induced near-surface currents. Figure 17(d) shows that some particles are also transported from the near-surface layer to the sub-surface layer. The major factors affecting the trajectories of particles are the phase of tide (flood or ebb) and the direction of local wind forcing in the Harbour during storm events. Particle tracking results are sensitive to the releasing time.

Hydrodynamic connectivity

To calculate the connectivity matrix from trajectories of passive particles, Halifax Harbour is divided into five subareas (Figure 1): Bedford Basin, the Narrows, Inner Harbour, Northwest Arm and Outer Harbour. A connectivity matrix is presented in Figure 18 based on the particle tracking experiments using the annual mean flow field. The horizontal and vertical elements in the connectivity matrix represent the sink and source region, respectively. The diagonal elements of the matrix from bottom-left to top-right

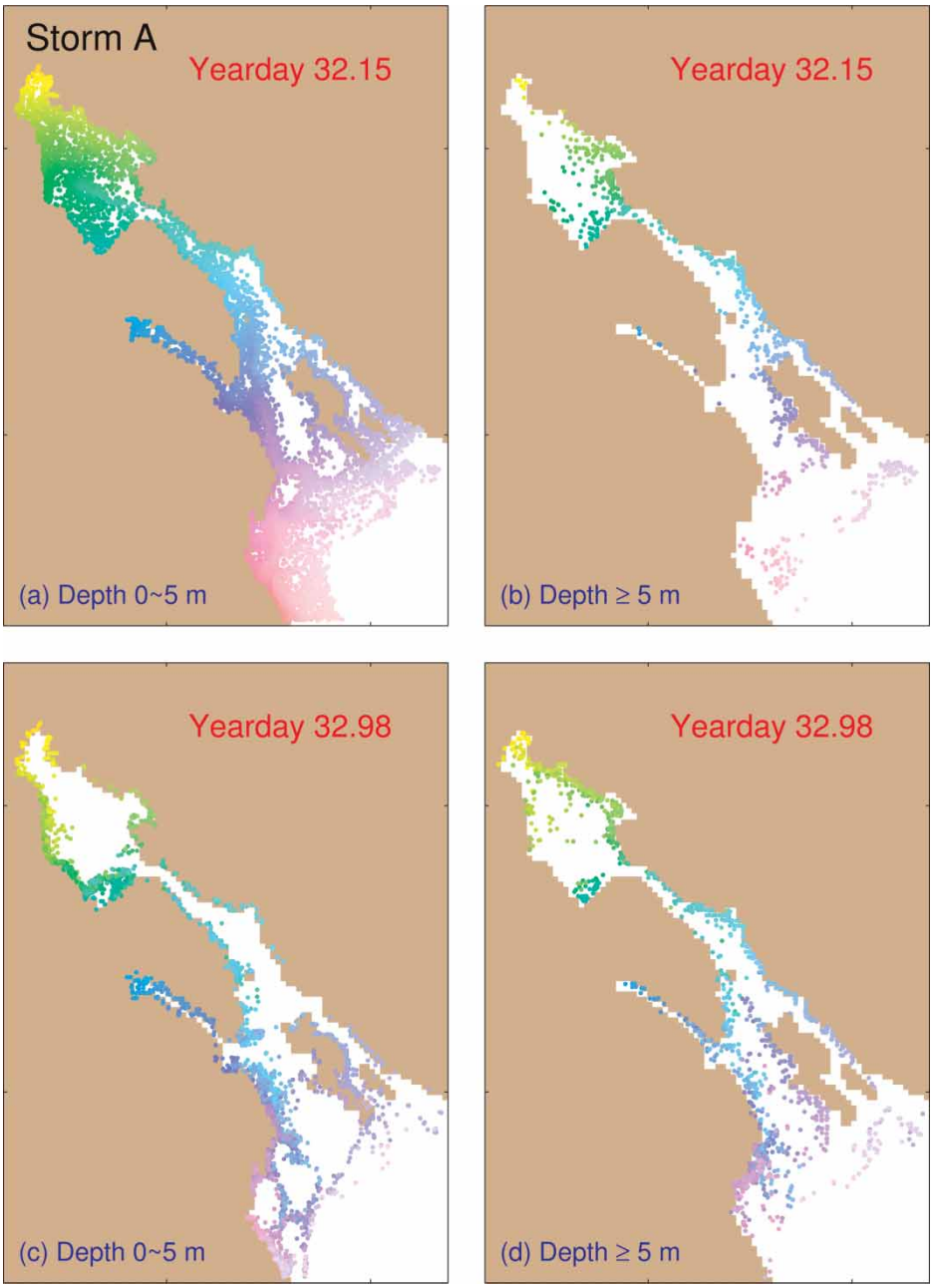

Figure 16 | Distributions of particles in (a), (c) the near-surface layer (0 ~ 5 m) and (b), (d) the sub-surface layer (≥5 m) 3.5 (a), (b) and 23.5 (c), (d) hours after the initial release in Halifax Harbour during storm A (yearday 32) in 2006. The 3D currents produced by submodel L5 during storm A with moderate diffusivity coefficients (A-m, Table 1) were used in the particle tracking.

represent percentages of particles remaining in their original subarea during the experiment period. The horizontal elements (S_h), with respect to each diagonal element (S_d) in the matrix, represent the percentages of the particles in a given subarea (S_d) reaching to other subareas (S_h, sink), and vertical elements (S_v) represent the percentages of the particles released in other subareas (S_v, source) moving to a given subarea (S_d) during the experiment period. For example, using the values in the connectivity matrix of experiment M-m (Figure 18), the hydrographic connectivity

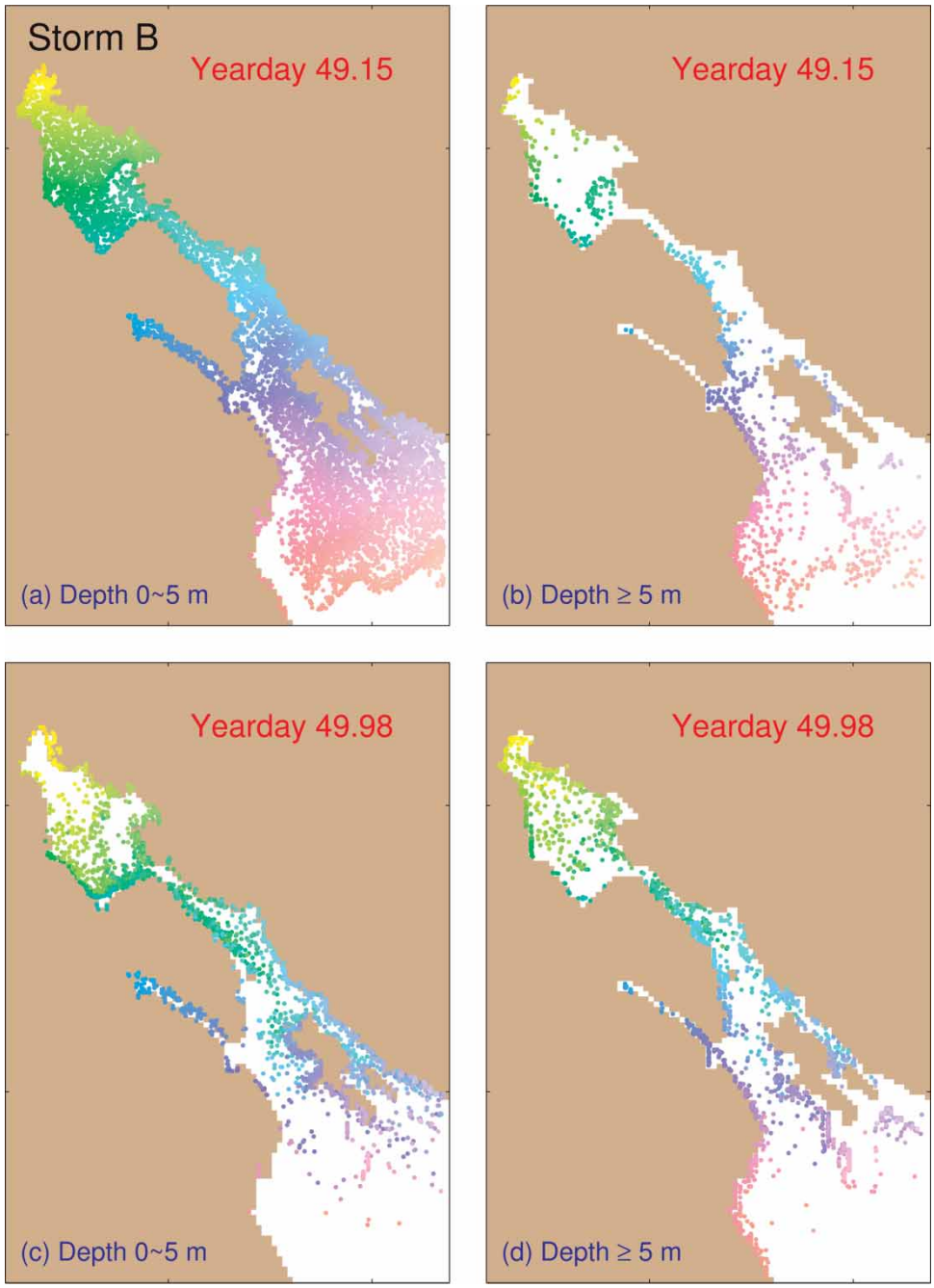

Figure 17 | Distributions of particles in (a), (c) the near-surface layer (0 ~ 5 m) and (b), (d) the sub-surface layer (≥5 m) 3.5 (a), (b) and 23.5 (c), (d) hours after the initial release in Halifax Harbour during storm B (yearday 49) in 2006. The 3D currents produced by submodel L5 during storm B with moderate diffusivity coefficients (B-m, Table 1) were used in the particle tracking.

of the Narrows related to other areas in the Harbour is presented in Figure 19, which can be easily understood by city planners and decision makers. About 79 and 87% of particles remain in Bedford Basin and the Northwest Arm, respectively, in experiment M-m (Figure 18). Nearly 90% of particles are flushed to the open sea in the Outer Harbour. About 21, 24 and 27% of particles travel from Bedford Basin to the Narrows, from the Narrows to the

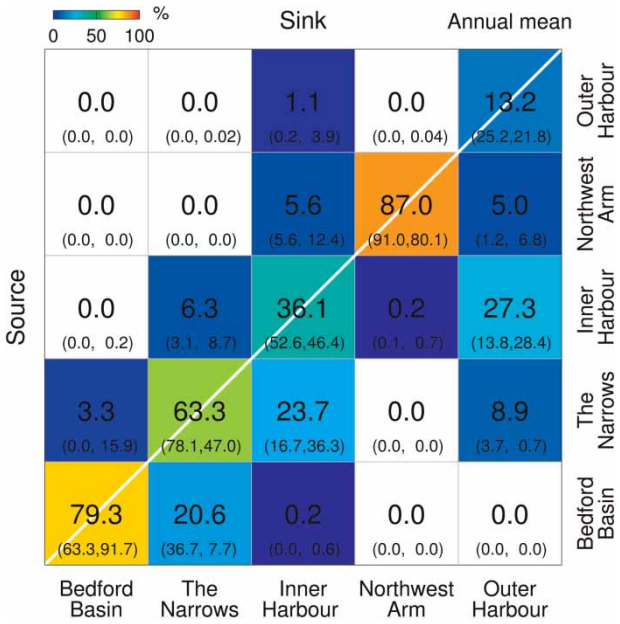

Figure 18 | Connectivity matrix over five subareas in Halifax Harbour (see Figure 1) based on the particle tracking experiments using the annual mean flow field produced by submodel L5. For each element, the centred value is from experiment M-m (see Table 1) with the moderate eddy diffusivities of the random walk process. The two numbers inside the round brackets are the values using low (left) and high (right) eddy diffusivities of the random walk process (experiments M-l and M-h). The centred value is used for the colour of each element. Please refer to the online version of this paper to see this figure in colour: http://www.iwaponline.com/wqrjc/toc.htm.

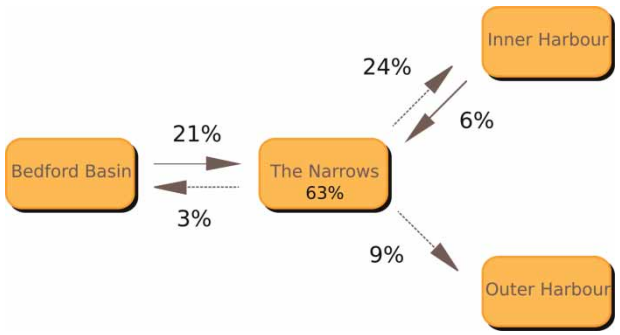

Figure 19 | Using the Narrows as an example to show how to interpret the connectivity matrix in Figure 18. Dashed and solid arrows indicate sink and source areas of the Narrows. Sixty-three percent of the particles initially released in the Narrows remain in the Narrows at the end of experiment M-m (5 days).

Inner Harbour, and from the Inner Harbour to the Outer Harbour, respectively, which indicates that the estuarine near-surface seaward currents carry particles from Bedford Basin to the open sea.

The connectivity matrices calculated from the particle tracking experiments using instantaneous flow fields during two storm events are shown in Figure 20. In the case of storm A, nearly all (99.7%) of the particles remain in Bedford Basin. More than 60% of particles initially over the Outer Harbour are flushed to the open ocean. For storm B, nearly 25% of particles released from Bedford Basin drift to other areas. More than 80% of the Outer Harbour's particles are flushed to the open ocean.

A sensitivity study on the role of eddy diffusivity coefficients of random walk in affecting the particle tracking results is presented in Figures 18 and 20. The overall connectivity patterns using the low (experiments M-l, A-l and B-l) and high (M-h, A-h and B-h) eddy diffusivity coefficients are similar to the results using moderate eddy diffusivity coefficients (M-m, A-m and B-m), indicating that advection is the dominant process in Halifax Harbour. The connectivity matrices also have some variations associated with different eddy diffusivity coefficients. Particles can be dispersed further away from their origins with larger eddy diffusivity coefficients, as expected. Generally, increasing eddy diffusivities decreases the retention (diagonal element) and enhances the strength of connectivity (off-diagonal element), which is demonstrated in the connectivity matrix during storm A (Figure 20). The connectivity matrix during storm B shows similar features, except for the connectivities among Bedford Basin, the Narrows and Inner Harbour.

SUMMARY AND DISCUSSION

A multi-nested coastal ocean circulation modelling system (DalCoast-HFX) was used in this study to simulate the storm-induced circulation in Halifax Harbour under extreme storm conditions. The flushing time and hydrodynamic connectivity in the Harbour were quantified for the first time, based on 3D model currents using both the Eulerian and Lagrangian approaches. DalCoast-HFX was driven by tides, water discharges, wind stress, atmospheric pressure at the sea level and surface heat fluxes. It was demonstrated that DalCoast-HFX is reasonably skilled in hindcasting the sea level variations, including tidal and non-tidal components, tidal currents, temperature and salinity in Halifax Harbour. The near-surface circulation under severe winter storms was discussed.

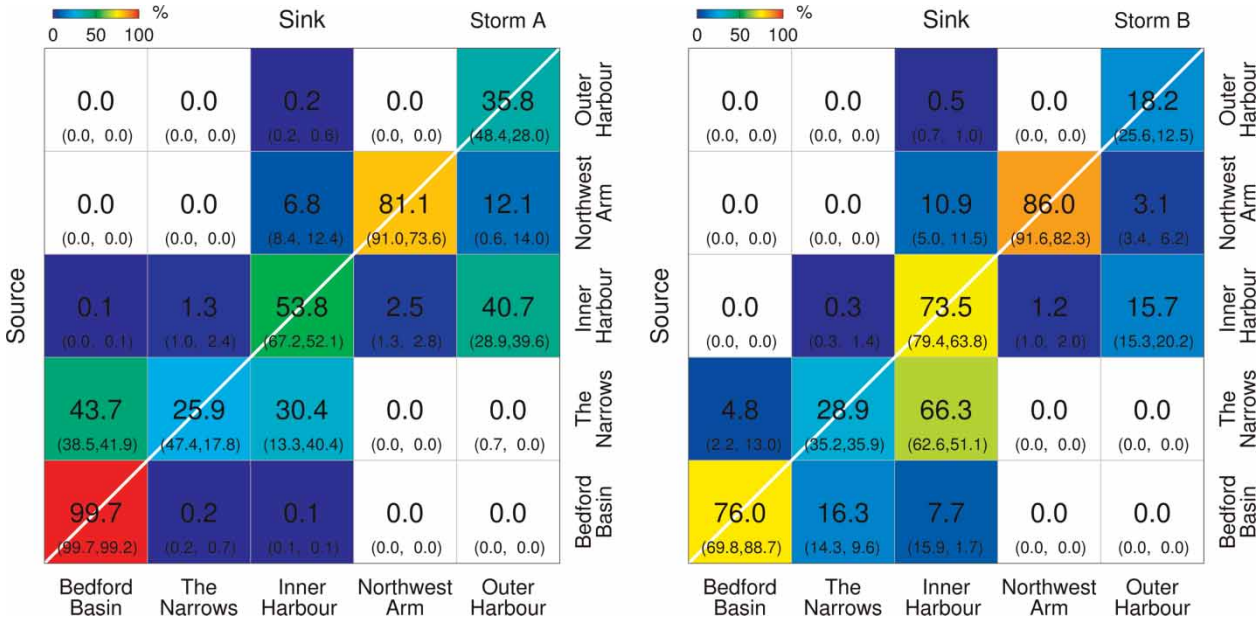

Figure 20 | Connectivity matrices over five subareas in Halifax Harbour (see Figure 1) based on the particle tracking experiments using instantaneous flow fields during storms A and B produced by submodel L5. For each element in the left [right] matrix, the centred value is from experiment A-m [B-m] (see Table 1) with the moderate eddy diffusivities of the random walk process. The two numbers inside the round brackets are the values using low (left) and high (right) eddy diffusivities of random walk process (experiments A-l and A-h [B-l and B-h]). The centred value is used for the colour of each element. Please refer to the online version of this paper to see this figure in colour: http://www.iwaponline.com/wqrjc/toc.htm.

Numerical passive tracer and particle tracking experiments were conducted to estimate the flushing time, dispersion and retention in Halifax Harbour. Based on model results in the passive tracer experiments, the flushing time was estimated to be about 90.6 days in the entire Bedford Basin, 39.2 days in the upper Bedford Basin, and less than 5 days in the Narrows, Inner Harbour and Outer Harbour.

Trajectories of particles carried passively by the model currents demonstrated that movements of passive particles in Halifax Harbour are strongly affected by tidal and storm-induced currents. Hydrodynamic connectivity in the study region was calculated in terms of a connectivity matrix. Under calm conditions, the particle tracking experiment shows that within 5 days, about 79 and 87% of the particles remain in Bedford Basin and the Northwest Arm, respectively, and nearly 90% of the particles are flushed to the open sea from the Outer Harbour. Under extreme conditions, the particle movements and hydrodynamic connectivity in the Harbour vary significantly in different storm events. A sensitivity study of the eddy diffusivity coefficients for the random walk process demonstrates that advection is the dominant process in dispersing particles in the Harbour. For most of the subareas, increasing eddy diffusivity can decrease the retention and enhance the connectivity.

The flow-induced movements of tracers and particles in Halifax Harbour were examined in this study. Apparently, characteristics of active tracers and particles, such as the chemical material, bacteria, phytoplankton and sediment, and their interaction with the environment, can cause the flushing time, dispersion and retention to be significantly different from the values estimated from passive tracers and particles. In a future study, biogeochemistry, such as bacterial decay, phytoplankton blooming and sediment settlement, can be included to obtain more realistic estimations of flushing time and dispersion in Halifax Harbour.

ACKNOWLEDGEMENTS

We thank Keith R. Thompson, David A. Greenberg, Brian Petrie, David B. Scott and Jocelyne Hellou for their constructive suggestions. Comments from two anonymous reviewers and the editor led to improvements in the manuscript. This research was supported by the Natural Sciences and Engineering Research Council of Canada

(NSERC), the Ocean Tracking Network Canada (OTN) and The Lloyd's Register Educational Trust (The LRET). The LRET is an independent charity working to achieve advances in transportation, science, engineering and technology education, training and research worldwide for the benefit of all.

REFERENCES

Ali, A., Thiem, Ø. & Berntsen, J. 2011 Numerical modelling of organic waste dispersion from fjord located fish farms. *Ocean Dynamics* **61**, 977–989.

Buckley, D. E. & Winters, G. V. 1992 Geochemical characteristics of contaminated surficial sediments in Halifax Harbour: impact of waste discharge. *Canadian Journal of Earth Sciences* **29** (12), 2617–2639.

Choi, K. & Lee, J. 2004 Numerical determination of flushing time for stratified water bodies. *Journal of Marine Systems* **50** (3), 263–281.

Durski, S., Glenn, S. & Haidvogel, D. 2004 Vertical mixing schemes in the coastal ocean: comparison of the level 2.5 Mellor-Yamada scheme with an enhanced version of the K profile parameterization. *Journal of Geophysical Research* **109** (C1), C01–C015.

Fournier, R. O. 1990 Halifax Harbour Task Force Final Report. Technical Report, Halifax, NS.

Greenberg, D. A. 1999 Atlas of Tidal Currents for Halifax Harbour. http://www2.mar.dfo-mpo.gc.ca/science/ocean/coastal_hydrodynamics/atlas/atlas.pdf (accessed 8 December 2011).

Huntsman, A. G. 1924 Circulation and pollution of water near and around Halifax Harbour. *Contributions to Canadian Biology* **2**, 71–81.

Mellor, G. & Yamada, T. 1982 Development of a turbulence closure model for geophysical fluid problems. *Reviews of Geophysics and Space Physics* **20** (4), 851–875.

Pawlowicz, R., Beardsley, B. & Lentz, S. 2002 Classical tidal harmonic analysis including error estimates in MATLAB using T_TIDE. *Computers and Geosciences* **28** (8), 929–937.

Petrie, B. & Yeats, P. 1990 Simple models of the circulation, dissolved metals, suspended solids and nutrients in Halifax Harbour. *Water Pollution and Resource Journal of Canada* **25** (3), 325–349.

Press, W., Teukolsky, S., Vetterling, W. & Flannery, B. 1992 *Numerical Recipes in Fortran: The Art of Scientific Computing*. Cambridge University Press, New York.

Riddle, A. & Lewis, R. 2000 Dispersion experiments in U.K. coastal waters. *Estuarine, Coastal and Shelf Science* **51** (2), 243–254.

Shan, S., Sheng, J., Thompson, K. R. & Greenberg, D. A. 2011 Simulating the three-dimensional circulation and hydrography of Halifax Harbour using a multi-nested coastal ocean circulation model. *Ocean Dynamics* **61** (7), 951–976.

Sheng, J., Wright, D., Greatbatch, R. & Dietrich, D. 1998 CANDIE: a new version of the DieCAST ocean circulation model. *Journal of Atmospheric and Oceanic Technology* **15**, 1414–1432.

Sheng, J., Zhao, J. & Zhai, L. 2009 Examination of circulation, dispersion, and connectivity in Lunenburg bay of Nova Scotia using a nested-grid circulation model. *Journal of Marine Systems* **77** (3), 350–365.

Signell, R. & Butman, B. 1992 Modeling tidal exchange and dispersion in Boston Harbor. *Journal of Geophysical Research* **97** (C10), 15,591–15,606.

Smagorinsky, J. 1963 General circulation experiments with the primitive equations. *Monthly Weather Review* **91**, 99–164.

Taylor, G. 1922 Diffusion by continuous movements. *Proceedings of the London Mathematical Society* **2** (1), 196–212.

Thompson, K. R. & Sheng, J. 1997 Subtidal circulation on the Scotian Shelf: assessing the hindcast skill of a linear, barotropic model. *Journal of Geophysical Research* **102** (C11), 24,987–25,003.

Thompson, K. R., Dowd, M., Shen, Y. & Greenberg, D. A. 2002 Probabilistic characterization of tidal mixing in a coastal embayment: a Markov chain approach. *Continental Shelf Research* **22** (11–13), 1603–1614.

Thompson, K. R., Ohashi, K., Sheng, J., Bobanovic, J. & Ou, J. 2007 Suppressing bias and drift of coastal circulation models through the assimilation of seasonal climatologies of temperature and salinity. *Continental Shelf Research* **27** (9), 1303–1316.

Tseng, R. S. 2002 On the dispersion and diffusion near estuaries and around islands. *Estuarine, Coastal and Shelf Science* **54** (1), 89–100.

Wilson, S. J. 2000 Case Study: the Costs and Benefits of Sewage Treatment and Source Control for Halifax Harbour. http://www.gpiatlantic.org/pdf/water/halharbour.pdf (accessed 8 December 2011).

Yang, B. & Sheng, J. 2008 Process study of coastal circulation over the inner Scotian Shelf using a nested-grid ocean circulation model, with a special emphasis on the storm-induced circulation during tropical storm Alberto in 2006. *Ocean Dynamics* **58** (5), 375–396.

First received 8 December 2011; accepted in revised form 5 September 2012